 CMES, vol.3, no.1, pp.53-63, 2002

A Meshless Local Petrov-Galerkin Method for Solving the Bending Problem of a Thin Plate

Shuyao Long[1], **S. N. Atluri**[2]

Abstract: Meshless methods have been extensively popularized in literature in recent years, due to their flexibility in solving boundary value problems. The meshless local Petrov-Galerkin(MLPG) method for solving the bending problem of the thin plate is presented and discussed in the present paper. The method uses the moving least-squares approximation to interpolate the solution variables, and employs a local symmetric weak form. The present method is a truly meshless one as it does not need a mesh, either for the purpose of interpolation of the solution or for the integration of the energy. All integrals can be easily evaluated over regularly shaped domains (in general, spheres in three-dimensional problems) and their boundaries. The essential boundary conditions are enforced by the penalty method. Several numerical examples are presented to illustrate the implementation and performance of the present method. The numerical examples presented in the paper show that high accuracy can be achieved for arbitrary nodal distributions for clamped and simply-supported edge conditions. No post processing procedure is required to compute the strain and stress, since the original solution from the present method, using the moving least squares approximation, is of C^2 type.

1 Introduction

Meshless methods have become very attractive and efficient for the development of adaptive methods for solving boundary value problems because nodes can be easily added and deleted without a burdensome remeshing of the entire structure [Kim and Atluri (2000)]. The main advantage of meshless methods is to get rid of or at least alleviate the difficulty of meshing and remeshing the entire structure. Recently, a meshless local Petrov-Galerkin (MLPG) approach (Atluri and Zhu (1998, 2000); Atluri, Kim, and Cho (1999b); Atluri, Cho, and Kim (1999a)], based on the local symmetric weak form over a local subdomain, and the shape function from the moving least-squares (MLS) approximation, has been successfully developed. The generality of the MLPG approach, based on either symmetric or unsymmetric weak-forms, and using 5 different types of meshless interpolations of trial functions, as well as 6 different types of meshless interpolation test functions, has been comprehensively discussed by Atluri and Shen (2002a, b).

The MLPG is a truly numerical meshless method for solving linear and non-linear boundary value problems, as no mesh is required in this method, either for purposes of interpolation of the solution variables, or for the integration of the energy. All integrals can be easily evaluated over regularly shaped domains (in general, spheres in three-dimension problems) and their boundaries.

The MLPG approach is also more flexible and easier in dealing with non-linear problems than the conventional FEM, EFG and BEM, as domain integrals will not cause any difficulty in implementing this method.

In the present work, the local Petrov-Galerkin approach will be developed for solving the bending problem of a thin plate. As has been illustrated in Atluri and Zhu (1998), and in Gu and Liu for plate problems (2001), the MLPG approach is a real meshless method, which needs absolutely no domain or boundary elements. Only domain and boundary integrals over very regular subdomains and their boundaries are involved in the formulation. These integrals are very easy to evaluate, due to the very regular shapes of the sub-domains (generally n-dimensional spheres) and their boundaries. The essential boundary condition in the MLPG approach is enforced, a posteriori, by a penalty formulation.

In the present paper, all explanations of terminology,

[1] Department of Engineering Mechanics
Hunan University
Changsha, Hunan 410082, P. R. China
[2] Center for Aerospace Research & Education,
48-121, Engineering IV,
7704 Boelter Hall,
University of California at Los Angeles, CA 90095-1600, USA

such as the support of a source point (node) ξ_i , the domain of definition of a MLS approximation for the trial function at any point *x*and the domain of influence of node ξ_i,are based on definitions in Atluri and Zhu (1998).

2 The meshless local Petrov-Galerkin (MLPG) approach for solving the bending problem of a thin plate

The MLPG approach is first proposed by Atluri and Zhu (1998) for solving linear potential problems. MLPG approach uses either a local symmetric weak form, or an unsymmetric weak-form as in the case of the Local Boundary Integral Equation method. The generality of the MPLG, based on either symmetric or unsymmetric weak-forms, and a variety of meshless trial and test functions, is discussed comprehensively in Atluri and Shen (2002a,b). In the present paper, we use the MLS approximation to develop a truly meshless method, based on a local symmetric weak-form. As the MLS approximation is used to construct shape functions, the essential boundary conditions in the MLPG approach are enforced, a posteriori, by a penalty formulation.

A standard Kirchhoff formulation of the plate equation, which results in a biharmonic equation in the transverse displacement, is used. The governing equation of the Kirchhoff plate in the transverse displacement may be written as

$$D\nabla^4 w(x_1,x_2) = q(x_1,x_2), (x_1,x_2) \in \Omega, \tag{1}$$

where $q(x_1,x_2)$is the prescribed distributed load per unit area normal to the plate, the $w(x_1,x_2)$is the plate deflection (along x_3 axis), and ∇^4 is a biharmonic operator, which may be written as in a Cartesian coordinate system

$$\nabla^4 = \frac{\partial^4}{\partial x_1^4} + 2\frac{\partial^4}{\partial x_1^2 \partial x_2^2} + \frac{\partial^4}{\partial x_2^2}, \tag{2}$$

D is the flexural rigidity being given as (E is the Young/s modulus, $\nu$is the Poisson constant, and h is the plate thickness)

$$D = \frac{Eh^3}{12(1-\nu^2)}. \tag{3}$$

The plate domain Ω is enclosed by Γ with the following boundary conditions:

The essential boundary conditions are:

$$w = \overline{w}, \quad \text{on} \quad \Gamma_{u1}; \tag{4}$$

$$\frac{\partial w}{\partial n} = \overline{\theta}_n, \quad \text{on} \quad \Gamma_{u2}. \tag{5}$$

The natural boundary conditions are:

$$M_n = \overline{M}_n, \quad \text{on} \quad \Gamma_{t1}; \tag{6}$$

$$V_n = \overline{V}_n, \quad \text{on} \quad \Gamma_{t2}. \tag{7}$$

where symbols $\overline{w}, \overline{\theta}_n, \overline{M}_n, \overline{V}_n$ denote the prescribed deflection, rotation angle about the tangent to the boundary Γ,bending moment and effective shear force, respectively, suffix n denotes the outward normal direction to the boundary Γ.

A generalized local weak form of the differential equation (1) and the boundary conditions (4) and (5), over a local subdomain $\Omega_s(\in \Omega)$,can be written as

$$\int_{\Omega_s} (D\nabla^4 w - q) v \mathrm{d}\Omega + \alpha_1 \int_{\Gamma_{u1}} (w - \overline{w}) v \mathrm{d}\Gamma + \alpha_2 \int_{\Gamma_{u2}} (\frac{\partial w}{\partial n} - \overline{\theta}_n) v \mathrm{d}\Gamma = 0, \tag{8}$$

where w and v are the trial and test functions, respectively, Γ_{u1} and Γ_{u2} is a part of the boundary $\partial\Omega_s$ of Ω_s, over which the essential boundary conditions are specified, and $\alpha_1, \alpha_2 (>> 1)$ are penalty parameters used to impose the essential boundary conditions.

Using Green's identity and the divergence theorem in equation (8) yield the following expression:

$$\int_{\Omega_s}\{D\nabla^2 w\nabla^2 v - D(1-\nu)[\frac{\partial^2 w}{\partial x_1^2}\frac{\partial^2 v}{\partial x_2^2}+\frac{\partial^2 w}{\partial x_2^2}\frac{\partial^2 v}{\partial x_1^2} - 2\frac{\partial^2 w}{\partial x_1\partial x_2}\frac{\partial^2 v}{\partial x_1\partial x_2}] - qv\}\mathrm{d}\Omega + \int_{\partial\Omega_s}[\frac{\partial v}{\partial n}M_n(w) - vV_n(w)]\mathrm{d}\Gamma + \sum_T [M_t(w)]^+_- v + \alpha_1\int_{\Gamma_{u1}}(w-\overline{w})v\mathrm{d}\Gamma + \alpha_2\int_{\Gamma_{u2}}(\frac{\partial w}{\partial n}-\overline{\theta}_n)v\mathrm{d}\Gamma = 0, \tag{9}$$

where $\partial\Omega_s$ is the boundary of the subdomain Ω_s and n is the outward unit normal to the boundary $\partial\Omega_s$.

The local boundary $\partial\Omega_s$ is further divided into two parts, i.e. $\partial\Omega_s = L_s\cup\Gamma_s$, where L_s is a part of $\partial\Omega_s$, on which no boundary conditions are specified; and Γ_s is also a part of $\partial\Omega_s$,over which boundary conditions are specified. Thus equation (9) can be written as

$$\int_{\Omega_s}\{D\nabla^2 w\nabla^2 v - D(1-\nu)[\frac{\partial^2 w}{\partial x_1^2}\frac{\partial^2 v}{\partial x_2^2}+\frac{\partial^2 w}{\partial x_2^2}\frac{\partial^2 v}{\partial x_1^2} - 2\frac{\partial^2 w}{\partial x_1\partial x_2}\frac{\partial^2 v}{\partial x_1\partial x_2}] - qv\}\mathrm{d}\Omega + \int_{L_s}[\frac{\partial v}{\partial n}M_n(w) - vV_n(w)]\mathrm{d}\Gamma + \int_{\Gamma_s}[\frac{\partial v}{\partial n}M(w) - vV_n(w)]\mathrm{d}\Gamma + \alpha_1\int_{\Gamma_{u1}}(w-\overline{w})v\mathrm{d}\Gamma + \alpha_2\int_{\Gamma_{u2}}(\frac{\partial w}{\partial n}-\overline{\theta}_n)v\mathrm{d}\Gamma + \sum_{\mathrm{T}}[M_t(w)]^+_- v, \tag{10}$$

The symbol $[M_t(\cdot)]^+_-$ denotes a value of the jump twisting moment at a corner, T is the number of corners. The meanings of other symbols in equation (10) are as follows:

$$\left.\begin{array}{l} M_n(w) = \frac{-D}{2}(1-\nu)[\frac{1+\nu}{1-\nu}\nabla^2 w \\ +\cos 2\beta L_1(w) + 2\sin 2\beta L_2(w)], \\ M_t(w) = D(1-\nu)[\frac{1}{2}\sin 2\beta L_1(w) \\ -\cos 2\beta L_2(w)], \\ V_n(w) = Q_n(w) + \frac{\partial M_t}{\partial s} \\ = -D\frac{\partial}{\partial n}(\nabla^2 w) + L_3(M_t). \end{array}\right\} \tag{11}$$

where

$$\left.\begin{array}{l} \nabla^2 = \frac{\partial^2}{\partial r^2} + \frac{1}{r}\frac{\partial}{\partial r} + \frac{1}{r^2}\frac{\partial^2}{\partial\theta^2}, \\ L_1 = \frac{\partial^2}{\partial r^2} - \frac{1}{r}\frac{\partial}{\partial r} - \frac{\partial^2}{r^2\partial\theta^2}, \\ L_2 = \frac{\partial}{\partial r}(\frac{1}{r}\frac{\partial}{\partial\theta}), \\ L_3 = -[\sin\beta\frac{\partial}{\partial r} - \cos\beta\frac{\partial}{r\partial\theta} \\ +(\frac{\cos\beta}{r} - \frac{1}{\rho})\frac{\partial}{\partial\beta}]. \end{array}\right\} \tag{12}$$

in which ρ is the radius of curvature of the boundary Γ_s, and ρ located on the convex side of a curve is assumed to be positive. n,tdenote the outward normal and tagent directions of a boundary curve, and r,θ are polar coordinate axes. β is a angle between the direction of $r$and the outward normal $n$of the boundary.

In the following development, the Petrov-Galerkin method is used. Unlike in the conventional Galerkin method in which the trial and the test functions are chosen from the same space, the Petrov-Galerkin method uses the trial and the test functions from different spaces. In particular, the test functions need not vanish on the boundary where the essential boundary conditions are specified. In the present work, the trial function w is approximated by the MLS approximation, while the test function v will be chosen from known functions.

As the test function is chosen from known functions, the above equation (10) can be further simplified by deliberately selecting the test function v and its normal derivative $\partial v/\partial n$ such that they vanish over L_s, the circle (for an internal node) or the circular arc (for a node on the global boundary Γ). This can be easily accomplished by using the weight function in the MLS approximation as also a test function, with the radius r_i of the support of the weight function being replaced by the radius r_0 of the local domain Ω_s, such that the test function and its normal derivative vanish on L_s. In general, no boundary conditions are enforced for an internal node, i.e. $L_s \equiv \partial\Omega_s$. While the weight function from the MLS scheme is used as the test function in the present paper, one may use

any one of a variety of test functions discussed in Atluri and Shen (2002a,b), in constructing alternate MLPG approaches for the plate problem. In particular, the use of a Heaviside step function as a test function, for the plate problem, appears to be a good choice. Results from such an MLPG approach, for the plate problem, will be presented shortly.

The integral term along Γ_s vanishes in equation (10), and the term in equation (10) representing the value of jumps at the boundary corners also vanishes, when there are no corners on local boundary L_s. Equation (10) becomes as

$$\begin{aligned}
&\int_{\Omega_s} \{D\nabla^2 w\nabla^2 v - D(1-\nu)[\frac{\partial^2 w}{\partial x_1^2}\frac{\partial^2 v}{\partial x_2^2} \\
&+ \frac{\partial^2 w}{\partial x_2^2}\frac{\partial^2 v}{\partial x_1^2} - 2\frac{\partial^2 w}{\partial x_1 \partial x_2}\frac{\partial^2 v}{\partial x_1 \partial x_2}] - qv\}\mathrm{d}\Omega \\
&+ \alpha_1 \int_{\Gamma_{u1}} (w-\overline{w})v\mathrm{d}\Gamma \\
&+ \alpha_2 \int_{\Gamma_{u2}} (\frac{\partial w}{\partial n} - \overline{\theta}_n)v\mathrm{d}\Gamma = 0. \qquad (13)
\end{aligned}$$

For a node on the global boundary Γ,$L_s$is a circular arc, on which the test function v and its normal derivative $\partial v/\partial n$ vanish, while Γ_s is a section of the global boundary Γ of the original problem domain, along which the test function and its normal derivative would not vanish any more. Further, Γ_s is divided into Γ_u and/or Γ_t,where Γ_u is a part, on which the essential boundary conditions (4) and /or (5) are also specified. Imposing the natural boundary conditions (6) and (7) in equation (10) we obtain

$$\begin{aligned}
&\int_{\Omega_s} \{D\nabla^2 w\nabla^2 v - D(1-\nu)[\frac{\partial^2 w}{\partial x_1^2}\frac{\partial^2 v}{\partial x_2^2} \\
&+ \frac{\partial^2 w}{\partial x_2^2}\frac{\partial^2 v}{\partial x_1^2} - 2\frac{\partial^2 w}{\partial x_1 \partial x_2}\frac{\partial^2 v}{\partial x_1 \partial x_2}] - qv\}\mathrm{d}\Omega \\
&+ \int_{\Gamma_{u1}} [\frac{\partial v}{\partial n}M_n(w) - vV_n(w)]\mathrm{d}\Gamma \\
&+ \int_{\Gamma_{u2}} [\frac{\partial v}{\partial n}M_n(w) - vV_n(w)]\mathrm{d}\Gamma \\
&+ \int_{\Gamma_{t1}} [\frac{\partial v}{\partial n}\overline{M}_n - vV_n(w)]\mathrm{d}\Gamma \\
&+ \int_{\Gamma_{t2}} [\frac{\partial v}{\partial n}M_n(w) - v\overline{V}_n]\mathrm{d}\Gamma \\
&+ \alpha_1 \int_{\Gamma_{u1}} (w-\overline{w})v\mathrm{d} \\
&+ \alpha_2 \int_{\Gamma_{u2}} (\frac{\partial w}{\partial n} - \overline{\theta}_n)v\mathrm{d}\Gamma \\
&+ \sum_T [M_t(w)]_-^+ v = 0. \qquad (14)
\end{aligned}$$

Rearranging equation (14) ,we obtain the following local symmetric weak form (LSWF) in the bending problem of a thin plate, as

$$\begin{aligned}
&\int_{\Omega_s} \{D\nabla^2 w\nabla^2 v - D(1-\nu)[\frac{\partial^2 w}{\partial x_1^2}\frac{\partial^2 v}{\partial x_2^2} \\
&+ \frac{\partial^2 w}{\partial x_2^2}\frac{\partial^2 v}{\partial x_1^2} - 2\frac{\partial^2 w}{\partial x_1 \partial x_2}\frac{\partial^2 v}{\partial x_1 \partial x_2}]\}\mathrm{d}\Omega \\
&+ \int_{\Gamma_{u1}} (\frac{\partial v}{\partial n}M_n(w) - vV_n(w)]\mathrm{d}\Gamma \\
&+ \int_{\Gamma_{u2}} (\frac{\partial v}{\partial n}M_n(w) - vV_n(w)]\mathrm{d}\Gamma \\
&- \int_{\Gamma_{t1}} vV_n(w)\mathrm{d}\Gamma + \int_{\Gamma_{t2}} \frac{\partial v}{\partial n}M_n(w)\mathrm{d}\Gamma \\
&+ \alpha_1 \int_{\Gamma_{u1}} wv\mathrm{d}\Gamma + \alpha_2 \int_{\Gamma_{u2}} \frac{\partial w}{\partial n}v\mathrm{d}\Gamma \\
&+ \sum_T [M_t(w)]_-^+ v = \int_{\Omega_s} qv\mathrm{d}\Omega \\
&- \int_{\Gamma_{t1}} \frac{\partial v}{\partial n}\overline{M}_n d + \int_{\Gamma_{t2}} v\overline{V}_n\mathrm{d}\Gamma \\
&+ \alpha_1 \int_{\Gamma_{u1}} \overline{w}vd\Gamma + \alpha_2 \int_{\Gamma_{u2}} \overline{\theta}_n vd\Gamma. \qquad (15)
\end{aligned}$$

3 The MLS approximation

This section gives a brief summary of the MLS approximation. For details of the MLS approximation, see Be-

lytschko , Lu and Gu (1994), Atluri and Zhu (1998).

Consider a sub-domain Ω_x, the neighborhood of a point $\mathbf{x}$, which is located in the problem domain Ω. To approximate the distribution of function w in Ω_x, over a number of randomly located nodes $\{\mathbf{x}_i\}, i = 1,2,\ldots,n$, the moving least square approximant $w^a(\mathbf{x})$ of w, $\forall \mathbf{x} \in \Omega_{\mathbf{x}}$, can be defined by

$$w^a(\mathbf{x}) = \mathbf{p}^T(\mathbf{x})\mathbf{a}(\mathbf{x}), \forall \mathbf{x} \in \Omega_{\mathbf{x}}, \mathbf{x} = [x_1, x_2]^T, \tag{16}$$

where $\mathbf{p}^T(\mathbf{x}) = [p_1(\mathbf{x}), p_2(\mathbf{x}), \ldots, p_m(\mathbf{x})]$ is a complete monomial basis of order m, and $\mathbf{a}(\mathbf{x})$ is a vector containing coefficients $a_j(\mathbf{x}), j = 1,2,\ldots,m$, which are functions of the space coordinates $\mathbf{x} = [x_1, x_2]^T$. For example, for a 2-D plate problem,

$$\mathbf{p}^T(\mathbf{x}) = [1, x_1, x_2], \text{linear basis}, m = 3; \tag{17a}$$

$$\begin{aligned}\mathbf{p}^T(\mathbf{x}) &= [1, x_1, x_2, x_1^2, x_1x_2, x_2^2],\\ &\text{quadratic basis}, m = 6.\end{aligned} \tag{17b}$$

The coefficient vector $\mathbf{a}(\mathbf{x})$ is determined by minimizing a weighted discrete L_2 norm, defined as

$$\begin{aligned}J(\mathbf{x}) &= \sum_{i=1}^{\mathbf{n}} g_i(\mathbf{x})[\mathbf{p}^T(\mathbf{x})\mathbf{a}(\mathbf{x}) - \hat{w}_i]^2\\ &= [\mathbf{P}\cdot\mathbf{a}(\mathbf{x}) - \hat{\mathbf{w}}]^{\mathbf{T}}\cdot\mathbf{G}\cdot[\mathbf{P}\cdot\mathbf{a}(\mathbf{x}) - \hat{\mathbf{w}}],\end{aligned} \tag{18}$$

where $g_i(\mathbf{x})$ is the weight function associated with node i, with $g_i(\mathbf{x}) > 0$ for all $\mathbf{x}$ in the support of $g_i(\mathbf{x})$, $\mathbf{x}_i$ denotes the value of $\mathbf{x}$ at node i, n is the number of nodes in Ω_x for which the weight functions $g_i(\mathbf{x}) > 0$, and the matrices $\mathbf{P}$ and $\mathbf{G}$ are defined as

$$\mathbf{P} = \begin{bmatrix} \mathbf{p^T}(\mathbf{x_1}) \\ \mathbf{p^T}(\mathbf{x}_2) \\ \cdots \\ \mathbf{p^T}(\mathbf{x}_n) \end{bmatrix} \tag{19}$$

$$\mathbf{G} = \begin{bmatrix} g_1(\mathbf{x}) & & & 0 \\ & g_2(\mathbf{x}) & & \\ & & \cdots & \\ 0 & & & g_n(\mathbf{x}) \end{bmatrix} \tag{20}$$

and

$$\hat{\mathbf{w}}^{\mathbf{T}} = [\hat{w}_1, \hat{w}_2, \cdots, \hat{w}_n]. \tag{21}$$

Here it should be noted that $\hat{w}_i, i = 1,2,\cdots,n$ in equations (18) and (4) are the fictitious nodal values, and not the nodal values of the unknown trial function $w^a(\mathbf{x})$ in general.

The stationarity of J in equation (18) with respect to $\mathbf{a}(\mathbf{x})$ leads to the following linear relation between $\mathbf{a}(\mathbf{x})$ and $\hat{\mathbf{w}}$.

$$\mathbf{A}(\mathbf{x})\mathbf{a}(\mathbf{x}) = \mathbf{B}(\mathbf{x})\hat{\mathbf{w}}, \tag{22}$$

Where matrices $\mathbf{A}(\mathbf{x})$ and $\mathbf{B}(\mathbf{x})$ are defined by

$$\begin{aligned}\mathbf{A}(\mathbf{x}) &= \mathbf{P^T}\mathbf{G}\mathbf{P} = \mathbf{B}(\mathbf{x})\mathbf{P}\\ &= \sum_{\mathbf{i}=1}^{n} g_i(\mathbf{x})\mathbf{p}(\mathbf{x}_i)\mathbf{p^T}(\mathbf{x}_i),\end{aligned} \tag{23}$$

$$\begin{aligned}\mathbf{B}(\mathbf{x}) &= \mathbf{P^T}\mathbf{G}\\ &= [g_1(\mathbf{x})\mathbf{p}(\mathbf{x}_1), g_2(\mathbf{x})\mathbf{p}(\mathbf{x}_2), \cdots, g_n(\mathbf{x})\mathbf{p}(\mathbf{x}_n)].\end{aligned} \tag{24}$$

The MLS approximation is well defined only when the matrix $\mathbf{A}$ in equation (5) is non-singular. It can be seen that this is the case if and only if the rank of $\mathbf{P}$ equals m. A necessary condition for a well-defined MLS approximation is that at least $m$weight functions are non-zero (i.e. $n \geq m$) for each sample point $\mathbf{x} \in \Omega$ and that the nodes in $\Omega_{\mathbf{x}}$ will not be arranged in a special pattern such as on a straight line. Here a sample point may be a nodal point under consideration or a quadrature point.

Solving for a $\mathbf{a}(\mathbf{x})$ from equation (5) and substituting it into equation (1) gives a relation which may be written as the form of an interpolation function similar to that used in the FEM, as

$$\begin{aligned}&w^a(\mathbf{x}) = \Phi^T(\mathbf{x})\cdot\hat{\mathbf{w}} = \sum_{\mathbf{i}=1}^{\mathbf{n}} \Phi_i(\mathbf{x})\hat{w}_i,\\ &w^a(\mathbf{x}_i) \equiv w_i \neq \hat{w}_i, \mathbf{x} \in \Omega_x,\end{aligned} \tag{25}$$

Where

$$\mathbf{\Phi^T}(\mathbf{x}) = \mathbf{p^T}(\mathbf{x})\mathbf{A}^{-1}(\mathbf{x})\mathbf{B}(\mathbf{x}), \tag{26}$$

or

$$\Phi_i(\mathbf{x}) = \sum_{j=1}^{m} p_j(\mathbf{x})[\mathbf{A}^{-1}(\mathbf{x})\mathbf{B}(\mathbf{x})]_{ji}. \tag{27}$$

$\Phi_i(\mathbf{x})$ is usually called the shape function of the MLS approximation, corresponding to nodal point $\xi_\mathbf{i}$. From equations (6) and (9), it may be seen that $\Phi_i(\mathbf{x}) = 0$ when $g_i(\mathbf{x}) = 0$. In practical applications, $g_i(\mathbf{x})$ is generally chosen such that it is non-zero over the support of nodal point $\xi_\mathbf{i}$. The support of the nodal point $\xi_\mathbf{i}$ is usually taken to be a circle of radius r_i, centered at $\xi_\mathbf{i}$. The fact $\Phi_i(\mathbf{x}) = 0$ for $\mathbf{x}$ not in the support of nodal point $\xi_\mathbf{i}$ preserve the local character of the Moving Least Square approximation.

The smoothness of the shape functions $\Phi_i(\mathbf{x})$ is determined by that of the basis functions and of the weight functions. Let $C^k(\Omega)$ be the space of k-th continuously differentiable functions. If $g_i(\mathbf{x}) \in C^k(\Omega)$ and $p_j(\mathbf{x}) \in C^l(\Omega), \quad i = 1,2,\ldots,n; j = 1,2,\ldots,m,$ then $\Phi_i(\mathbf{x}) \in C^r(\Omega)$ with $r = \min(k,l)$.

The partial derivatives of $\Phi_i(\mathbf{x})$ are obtained as

$$\Phi_{i,k} = \sum_{j=1}^{m} [p_{j,k}(\mathbf{A}^{-1}\mathbf{B})_{ji} + p_j(\mathbf{A}^{-1}\mathbf{B}_{,k} + \mathbf{A}^{-1}_{,k}\mathbf{B})_{\mathbf{ji}}], \tag{28}$$

$$\begin{aligned}\Phi_{i,kl} = \sum_{j=1}^{m} [&p_{j,kl}(\mathbf{A}^{-1}\mathbf{B})_{ji} + p_{j,k}(\mathbf{A}^{-1}_{,l}\mathbf{B} \\ &+ \mathbf{A}^{-1}\mathbf{B}_{,l})_{ji} + p_{j,l}(\mathbf{A}^{-1}_{,k}\mathbf{B} + \mathbf{A}^{-1}\mathbf{B}_{,k})_{ji} \\ &+ p_j(\mathbf{A}^{-1}_{,kl}\mathbf{B} + \mathbf{A}^{-1}_{,k}\mathbf{B}_{,l} + \mathbf{A}^{-1}_{,l}\mathbf{B}_{,k} + \mathbf{A}^{-1}\mathbf{B}_{,kl})_{ji}],\end{aligned} \tag{29}$$

$$\begin{aligned}\Phi_{i,klr} = \sum_{j=1}^{m} [&p_{j,klr}(\mathbf{A}^{-1}\mathbf{B})_{ji} + p_{j,kl}(\mathbf{A}^{-1}_{,r}\mathbf{B} \\ &+ \mathbf{A}^{-1}\mathbf{B}_{,r})_{ji} + p_{j,lr}(\mathbf{A}^{-1}_{,k}\mathbf{B} + \mathbf{A}^{-1}\mathbf{B}_{,k})_{ji} \\ &+ p_{j,kr}(\mathbf{A}^{-1}_{,l}\mathbf{B} + \mathbf{A}^{-1}\mathbf{B}_{,l})_{ji} + p_{j,k}(\mathbf{A}^{-1}_{,lr}\mathbf{B} \\ &+ \mathbf{A}^{-1}_{,l}\mathbf{B}_{,r} + \mathbf{A}^{-1}_{,r}\mathbf{B}_{,l} + \mathbf{A}^{-1}\mathbf{B}_{,lr})_{ji} \\ &+ p_{j,l}(\mathbf{A}^{-1}_{,kr}\mathbf{B} + \mathbf{A}^{-1}_{,k}\mathbf{B}_{,r} + \mathbf{A}^{-1}_{,r}\mathbf{B}_{,k} + \mathbf{A}^{-1}\mathbf{B}_{,kr})_{ji} \\ &+ p_{j,r}(\mathbf{A}^{-1}_{,kl}\mathbf{B} + \mathbf{A}^{-1}_{,k}\mathbf{B}_{,l} + \mathbf{A}^{-1}_{,l}\mathbf{B}_{,k} + \mathbf{A}^{-1}\mathbf{B}_{,kl})_{ji} \\ &+ p_j(\mathbf{A}^{-1}_{,klr}\mathbf{B} + \mathbf{A}^{-1}_{,kl}\mathbf{B}_{,r} + \mathbf{A}^{-1}_{,kl}\mathbf{B}_{,l} + \mathbf{A}^{-1}_{,lr}\mathbf{B}_{,k} \\ &+ \mathbf{A}^{-1}_{,k}\mathbf{B}_{,lr} + \mathbf{A}^{-1}_{,l}\mathbf{B}_{,kr} + \mathbf{A}^{-1}_{,r}\mathbf{B}_{,kl} + \mathbf{A}^{-1}\mathbf{B}_{,klr})_{ji}],\end{aligned}$$

$$(k,l,r = 1,2). \tag{30}$$

in which $\mathbf{A}^{-1}_{,k} = (\mathbf{A}^{-1})_{,k}$ represents the derivative of the inverse of $\mathbf{A}$ with respect to x_k, which is given by

$$\mathbf{A}^{-1}_{,k} = -\mathbf{A}^{-1}\mathbf{A}_{,k}\mathbf{A}^{-1}, \tag{31}$$

where, $(\cdot)_{,i}$ denotes $\partial(\cdot)/\partial x_i$. $\mathbf{A}^{-1}_{,kl}$ and $\mathbf{A}^{-1}_{,klr}$ are similar to $\mathbf{A}^{-1}_{,k}$.

4 Discretization and numerical implementation

Here transverse deflection w is interpolated using MLS approximation, i.e.

$$w^a(x) = \mathbf{\Phi}\hat{\mathbf{W}} = \sum_{j=1}^{N} \phi_j(x)\hat{w}_j, \tag{32}$$

where w_j is the unknown fictitious nodal values, N is the total number of nodes in a local domain Ω_s for which the weight functions $g_i(x) > 0$.

The shape functions of internal forces are obtained using equation (11)

$$M^a_n(x) = \sum_{j=1}^{N} M_{nj}(x)\hat{w}_j, \tag{33}$$

$$M^a_t(x) = \sum_{j=1}^{N} M_{tj}(x)\hat{w}_j, \tag{34}$$

$$V^a_n(x) = \sum_{j=1}^{N} V_{nj}(x)\hat{w}_j, \tag{35}$$

where

$$M_{nj}(x) = -D[\nu\phi_{j,pp} + (1-\nu)n_k n_l \phi_{j,kl}], \tag{36}$$

$$M_{tj}(x) = -D(1-\nu)(-1)^l n_k n_{3-l}\phi_{j,kl}, \tag{37}$$

$$\begin{aligned}V_{nj}(x) = -D[&\phi_{j,ppk}n_k + (1-\nu)(-1)^{l+m} \\ &n_k n_{3-l} n_{3-m}\phi_{j,klm}].\end{aligned} \tag{38}$$

in equations (36)$\sim$(38),$p,k,l,m = 1,2$.

In implementing the MLS approximation for transverse deflection w, the basis functions and weight functions

should be chosen at first. Both Gaussian and spline weight functions with compact supports can be considered. For the MLPG approach of the thin plate problem, the weight function in the MLS approximation is chosen as a test function, with the radius r_i of the support of the weight function being replaced by radius r_0 of the local domain of Ω_s, such that the test function and its normal derivative vanish on L_s. The spline weight function possesses the above required properties, but for the Gaussian weight function there are not those properties, as the normal derivative of the Gaussian weight function does not vanish on L_s. It should be noted that there exists the third order derivative in equation (15) at the boundaries of supports of sub-domain Ω_s, but the derivatives of the quartic spline weight function, higher than the second order, are discontinuous at the boundaries of supports of sub-domain Ω_s. In this work, the quintic spline weight function is considered for the MLPG approach of the thin plate problem.

A quintic spline weight function is defined as

$$g_i(x)=\begin{cases} 1-10(\frac{d_i}{r_i})^2+20(\frac{d_i}{r_i})^3-15(\frac{d_i}{r_i})^4+4(\frac{d_i}{r_i})^5, \\ \qquad\qquad 0\le d_i\le r_i; \\ 0, \qquad\qquad d\ge r_i. \end{cases} \tag{39}$$

where $d_i=\|x-x_i\|$,and r_i is the size of the support for the weight function g_i and determines the support of node x_i.

Substituting equations (32)$\sim$(35) into equation (15) for boundary node on the global boundary Γ and equation (13) for internal nodes. Leads to the following discretized system of linear equations:

$$\sum_{j=1}^{N}\mathbf{K}_{ij}\hat{\mathbf{w}}_j=\mathbf{f}_i, i=1,2,\cdots,N, \tag{40}$$

where N is the total number of nodes,

$$\begin{aligned}\mathbf{K}_{ij}=&\int_{\Omega_s}[D\phi_{j,kk}g_{i,ll}-D(1-\nu)(-1)^{k+l}\phi_{j,kl}g_{i,(3-k)(3-l)}]\mathrm{d}\Omega\\ &+\int_{\Gamma_{u1}}[\frac{\partial g_i}{\partial n}M_{nj}-g_iV_{nj}]\mathrm{d}\Gamma+\int_{\Gamma_{u2}}[\frac{\partial g_i}{\partial n}M_{nj}-g_iV_{nj}]\mathrm{d}\Gamma\\ &-\int_{\Gamma_{t1}}g_iV_{nj}\mathrm{d}\Gamma+\int_{\Gamma_{t2}}\frac{\partial g_i}{\partial n}M_{nj}\mathrm{d}\Gamma\\ &+\alpha_1\int_{\Gamma_{u1}}\phi_jg_i\mathrm{d}\Gamma+\alpha_2\int_{\Gamma_{u2}}\phi_{j,n}g_i\mathrm{d}\Gamma+\sum_T[\mathbf{M}_{tj}]^+_-g_i,\end{aligned} \tag{41}$$

$$\begin{aligned}\mathbf{f}_i=&\int_{\Omega_s}qg_i\mathrm{d}\Omega-\int_{\Gamma_{t1}}\frac{\partial g_i}{\partial n}\overline{M}_n\mathrm{d}\Gamma+\int_{\Gamma_{t2}}g_i\overline{V}_n\mathrm{d}\Gamma\\ &+\alpha_1\int_{\Gamma_{u1}}g_i\overline{w}\mathrm{d}\Gamma+\alpha_2\int_{\Gamma_{u2}}\overline{\theta}_ng_i\mathrm{d}\Gamma.\end{aligned} \tag{42}$$

in which $g_i=g_i(x)=g(x,x_i)$and is the value of the weight function, corresponding to node *i*,evaluated at the point *x*. It should be noted that for those interior nodes located inside the domain $\Omega, L_s\equiv\partial\Omega_s$, and the boundary integrals involving Γ_{u1},Γ_{u2} and Γ_{t1},Γ_{t2} vanish in equations (10) and (42).

Here, it should also be noted that two among the four boundary integrals involving Γ_{u1},Γ_{u2} and Γ_{t1},Γ_{t2} are chosen according the boundary conditions of the considered problem. If there exist corners on the boundary Γ of the considered problem, the term involving $\sum_T[M_{tj}]^+_-g_i$ in equation (10) should also be chosen. For example, two boundary integrals involving Γ_{u1} and Γ_{t1} should be chosen for a plate with all edges simply-supported.

5 Numerical examples

The square plate under various loads is a well-known benchmark with a large number of numerical and analytical solutions to compare with. The present results were compared with results of the global boundary element method (Costa, 1986), and analytical method(Timoshenko & Woinowsky-Krieger, 1959).

The basis functions and the weight functions are chosen at first in implementing the MLS approximation for the MLPG approach. In the present computation, cubic [m=10], quartic [m=15] and quintic [m=21] bases, as

well as the quintic spline weight function are employed to ensure the desired C^1 continuity within the support, as well as C^2 continuity on its boundary in equations (41) and (42). The resulting approximation is governed by the continuity of the weigh function. Due to the properties of the quintic spline weight function, C^2 trial functions are constructed. Thus, smooth moments can be obtained without any re-interpolation or smoothing.

In the formulation, the size of each local sub-domain should be big enough such that the union of all local sub-domains covers as much as possible of the global domain. In all the following examples, the size (radius) of the local sub-domain of each internal node is taken as the 2.5 times minimum nodaldistance, and that of each boundary node is taken as the 2.5 times maximum nodal distance. In the computation, 9 Gauss points are used on each section of Γ_s, and 6×9 points are used in each local domain Ω_s for numerical quadratures.

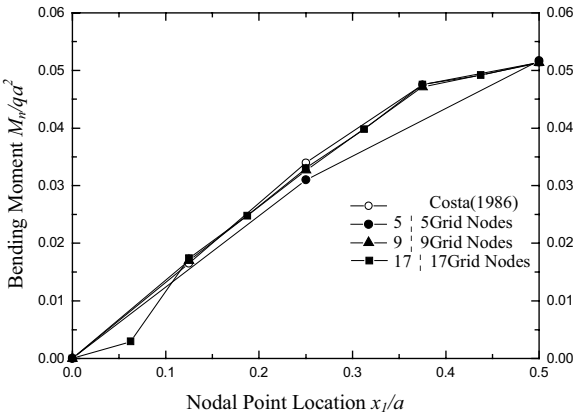

Figure 1 : Bending moment on half an edge of a uniformly loaded square plate with all edges clamped

5.1 A square plate with all edges clamped

A square plate subjected to a uniformly distributed load with all edges clamped is analyzed firstly to verify the reliability of the present method. Regular meshes of $25(5 \times 5), 81(9 \times 9), 289(17 \times 17)$ nodes (full plate) are used to compare with Costa's (1986) results. Table.1 provides results of the present method for the central deflection and some important bending moments. It can be seen from this table that the present results are in excellent agreement, contrast with those obtained by Costa (1986) using the global boundary element method and quoted by Timoshenko et al. (1959), which are also appear in this table.

In Table 1 the quartic basis and quintic spline weight function are used for present method, and linear boundary elements with 32 boundary nodes of full plate are employed for Costa (1986).The meanings of symbols in Table 1 are: q is a uniform load distribution, a is the side length of a square plate, $D$is the flexural rigidity of equation (3). Because of the symmetry, results of the bending moment and equivalent shear force on the boundary are presented for only half of one edge of the plate in Fig.1 and 2. As can be appreciated from the graphs in these figures, the results obtained by the present method for all grid nodes, even for 5×5 grid nodes, are in good agreement , compared with those given by Costa (1986).

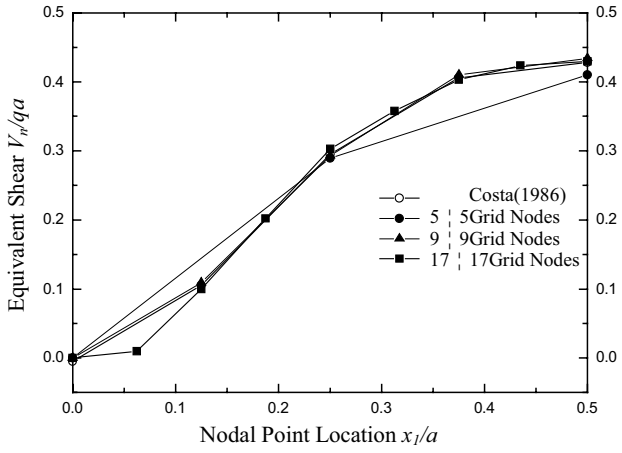

Figure 2 : Equivalent shear on half an edge of a uniformly loaded square plate with all edges clamped

Table 1 : Deflections and bending moments in a uniformly loaded squate plate with all edges clamped

Method		Deflection at the center ($\times D/qa^4$)	Bending moment at the center ($\times 1/qa^2$)	Bending moment at half of the edge($\times 1/qa^2$)
Present method	5×5	0.001250	0.02275	0.05170
	9×9	0.001253	0.02280	0.05145
	17×17	0.001257	0.02288	0.05142
Costa (1986)		0.01255	0.02282	0.05140
Timoshenko (1959)		0.01260	0.02310	0.05130

5.2 A square plate with all edges simply-supported

A square plate subjected a uniformly distributed load with all edges simply-supported is analyzed to illustrate the convergence of the present method. For the purpose of error estimation and convergence studies, the deflection and energy norm, $\|w\|$ and $\|e\|$,are calculated, These norms are defined as

$$\|w\| = [\int_\Omega w^2 \mathrm{d}\Omega]^{\frac{1}{2}}, \tag{43}$$

$$\|e\| = [\frac{D}{2}\int_\Omega (\nabla^2 w)^2 \mathrm{d}\Omega]^{\frac{1}{2}}. \tag{44}$$

The relative error for $\|w\|$ and $\|e\|$ are defined as

$$r_w = \frac{\|w^n - w^e\|}{\|w^e\|}, \tag{45}$$

$$r_e = \frac{\|e^n - e^e\|}{\|e^e\|}, \tag{46}$$

where $\|w\|$ and $\|e\|$ denote the numerical deflection and the strain energy obtained by the present method, respectively. w^e and e^e denote the exact deflection and the energy by the analytical method (Timosheuko & Woinowsky-Krieger, 1959), respectively, for which the exact solution of the deflection is

$$w = \frac{16q}{\pi^6 D}\sum_{m=1,3,\cdots}^{\infty}\sum_{n=1,3,\cdots}^{\infty}\frac{\sin\frac{m\pi x}{a}\sin\frac{n\pi y}{a}}{mn(\frac{m^2}{a^2}+\frac{n^2}{a^2})}, \tag{47}$$

where q is a uniformly distributed load, and a is the side length of a square plate.

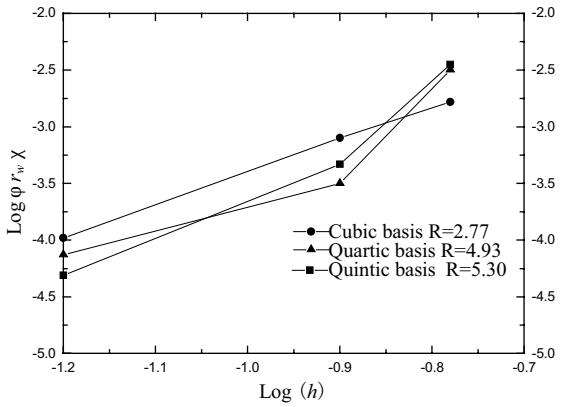

Figure 3 : Relative errors and convergence rates for deflection norm $\|w\|$ for the square plate with all edges simply-supported.

Regular meshes of $49(7\times 7)$, $81(9\times 9)$ and $289(17\times 17)$ nodes are used, and the MLS approximation with Cubic, quartic and quintic basis as well as the quintic spline weight function are employed in the computation.

The convergence with mesh refinement of the present method is studied for this problem. The results of relative errors and convergence rates are shown in Figures 3 and 4 for deflection and strain energy, respectively. These figures show that the present meshless method based the MLPG approach has high rates of convergence for norms $\|w\|$ and $\|e\|$, and give reasonably accurate results for the unknown deflection and its derivatives.

In this example, it can be seen that the quintic basis yields somewhat of a better result than the cubic and quartic bases while three bases possess high accuracy.

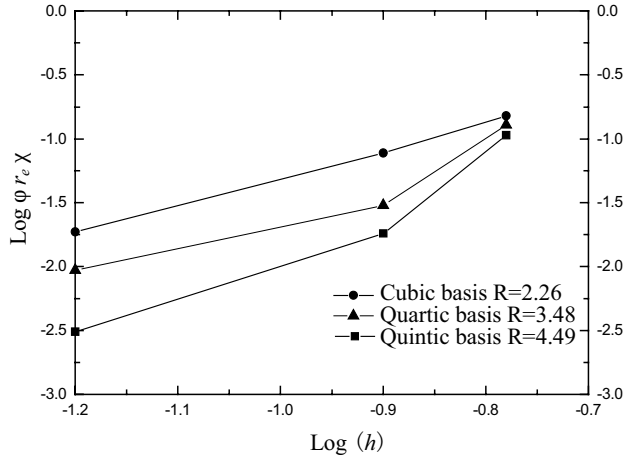

Figure 4 : Relative errors and convergence rates for energy norm $||e||$ for the square plate with all edges simply-supported.

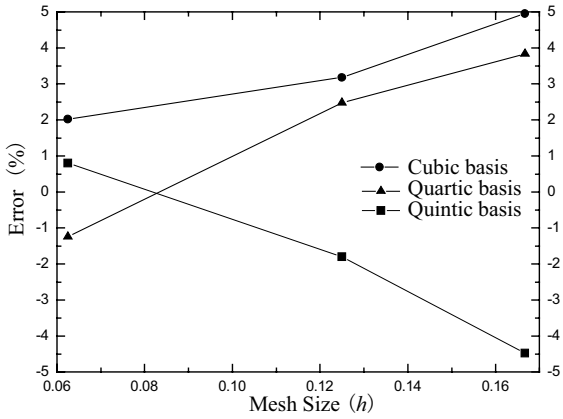

Figure 5 : Convergence with mesh refinement for different basis

5.3 Convergence of the central deflection for different basis

A square plate with all edges simply-supported under central force is here solved to study the convergence of deflections. Regular meshes of 49(7×7),81(9×9) and 289(17×17)nodes are used, and the MLS approximation with cubic, quartic and quintic bases, as well as the quintic spline weight functions are employed in the computation.

The convergence with mesh refinement of the present method is studied for this problem. The results are shown in Fig.5. It can be seen that the present meshless method based upon the MLPG approach has high rates of convergence for the central deflections and gives reasonably accurate results. It can also be noted that quintic basis function gives also higher accuracy.

6 Conclusions

The basic concept and implementation of the MLPG approach for solving thin (Kirchhoff) plates have been presented in the present work. The numerical implementation of the approach may lead to an efficient meshless discrete model. Convergence studies in the numerical examples show that the present method possesses an excellent rate of convergence for the deflection and strain energy. Only a simply numerical manipulation is need for calculating internal forces, as the original approximated trial solution is smooth enough to yield reasonably accurate results for internal forces. numerical results show that using the quintic spline weight function, and the quintic basis in approximation function, can give quite accurate numerical results.

While the finite element construction of C^1 numerical approximation is difficult and unsatisfactory so far, and while various devices to avoid the need for C^1 ab initio are employed (discrete Kirchhoff theory, hybrid stress, or even transition to C^0 theory), the current moving least square method achieves C^1 and even C^2 approximations in a very straightforward manner.

Isotropic material law and uniform plate thickness were assumed for simplicity in the present work, the results apply directly to any material law and any thickness variation, however. Besides, the current formulation possesses flexibility in adapting the density of the nodal points at any place of the problem domain such that the resolution and fidelity of the solution can be improved easily. This is especially useful in developing intelligent, adaptive algorithms based on error indicators for engineering applications.

Acknowledgement: This work was supported by the National Natural Science Foundation of China (No. 19972019). The second author acknowledges the support of NASA Lanpley Research Center, and the encouragement of Dr. I.G. Raju.

References

Atluri, S.N. and Shen, S. (2002a): *The Meshless Local Petrov-Galerkin (MLPG) Method.* Tech Science press, 382 pages.

Atluri, S.N. and Shen, S. (2002b): The Meshless Local Petrov-Galerkin (MLPG) Method: A Simple & Less-Costly Alternatifve to the Finite Element and Boundary Element Methods. *CMES: Computer Modeling in Engineering & Sciences*, vol. 3, No. 1, pp. 11-53.

Atluri, S.N. and Zhu, T.(1998): A new meshless local Petrov-Galerkin (MLPG) approach in computational mechanics. *Comput. Mech.* 22:117∼127

Atluri, S.N.; Cho, J.Y.; Kim, H.G.(1999a): Analysis of thin beams, using the meshless local Petrov-Galerkin method, with generalized moving least squares interpolation. *Comput. Mech* .24:334∼347

Atluri, S.N.; Kim, H.G.; Cho, J.Y. (1999b): A critical assessment of the truly meshless local Petrov-Galerkin (MLPG), and local boundary integral equation (LBIE) methods. *Comput. Mech* .24:348∼372

Atluri, S.N., and Zhu, T. (2000): New concepts in meshless methods. International Journal for Numerical Methods in Engineering. 47:537∼556

Belytschko, T.; Lu, Y.Y.; Gu, L.(1994): Element-free Galerkin methods. *International Journal for Numerical Methods in Engineering.* 37:229∼256

Costa, JA(1986): The boundary element method applied to plate problems. PhD thesis, Southampton University, Southampton, UK

Gu, Y.T. and Liu, G.R. (2001): A Meshless Local Petrov-Galerkin (MLPG) Formulation for Static and Free Vibration Analyses of Thin Plates, *CMES: Computer Modeling in Engineering & Sciences*, vol. 2, no. 4, pp 463-476.

Kim, H.G. and Atluri, SN (2000): Arbitrary Placement of Secondary Nodes, and Error Control, in the Meshless Local Petrov-Galerkin (MLPG) Method, *CMES: Computer Modeling in Engineering & Sciences*, vol. 1, no. 3, pp. 11-32.

Timoshenko, S. and Woinowsky-Krieger, S. (1959): Theory of Plates and shells. 2nd ed. McGraw-Hill, New York